Electronic Supplementary Material (ESI) for Journal of Materials Chemistry A.
This journal is © The Royal Society of Chemistry 2018

Supplementary Information

A universal strategy for the *in-situ* synthesis of TiO_2(B) nanosheets on pristine carbon materials for high-rate lithium storage

Long Pan,[a] Zheng-Wei Zhou,[a] Yi-Tao Liu*[b] and Xu-Ming Xie*[a]

[a] Laboratory of Advanced Materials (MOE), Department of Chemical Engineering, Tsinghua University, Beijing 100084, China

[b] State Key Laboratory of Organic−Inorganic Composites, Beijing Key Laboratory of Electrochemical Process and Technology for Materials, Beijing University of Chemical Technology, Beijing 100029, China

*E-mail: liu-yt03@mails.tsinghua.edu.cn; xxm-dce@mail.tsinghua.edu.cn

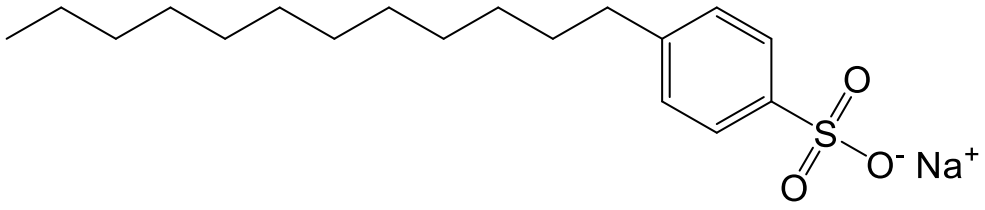

Fig. S1 Molecular structure of SDBS.

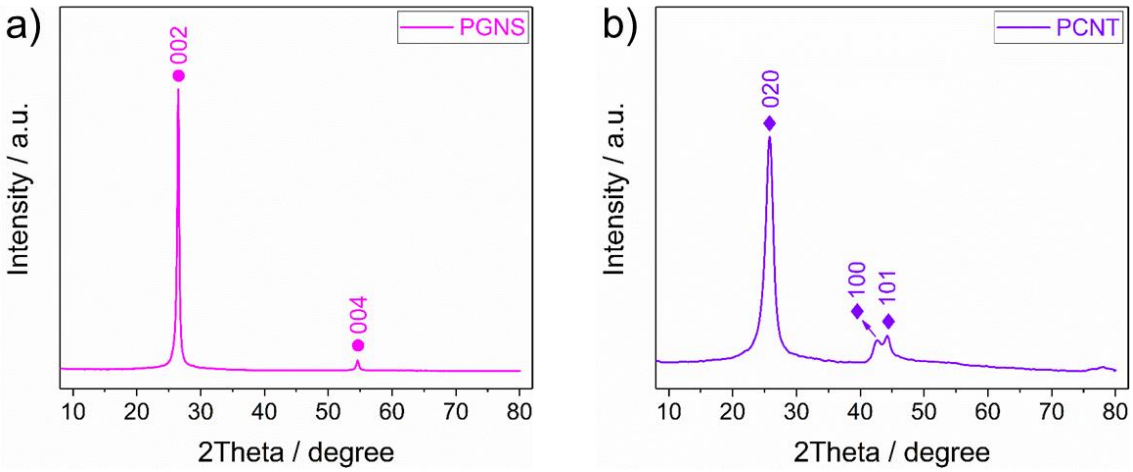

Fig. S2 XRD patterns of (a) PGNS and (b) PCNT.

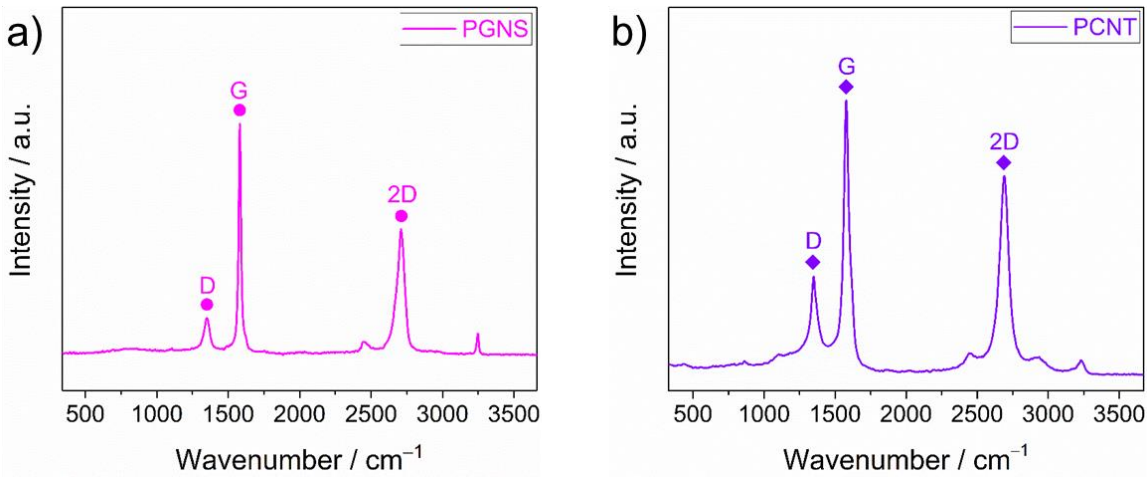

Fig. S3 Raman spectra of (a) PGNS and (b) PCNT. For graphene and CNT, the D peak is considered as defect-induced Raman band, and the G peak is considered as defect-free (sp^2 C atoms) Raman band.[1] The intensity ratio ($r = I_D/I_G$) of the D band and G band usually represents the degree of defects in graphene and CNT.[1-3] The smaller the value of r, the fewer the defects. The r values of PGNS and PCNT are 0.25 and 0.29, respectively, which are dramatically lower than those of r-GO and r-CNT (generally, $r > 1$),[1] indicating the highly ordered structure of PGNS and PCNT. As a result, PGNS and PCNT have much better conductivity than r-GO and r-CNT.

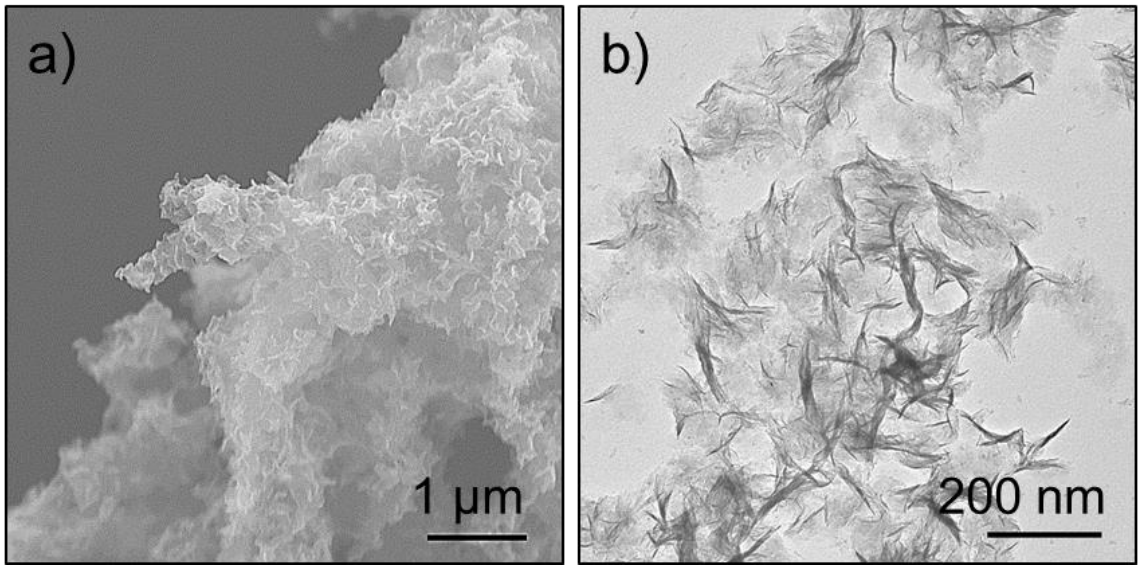

Fig. S4 (a) SEM and (b) TEM images of TiO_2(B) nanosheets. These TiO_2(B) nanosheets were synthesized in the absence of PGNS or PCNT. It is clearly seen from TEM image that the lateral sizes of these TiO_2(B) nanosheets are small (about several hundred nanometers).

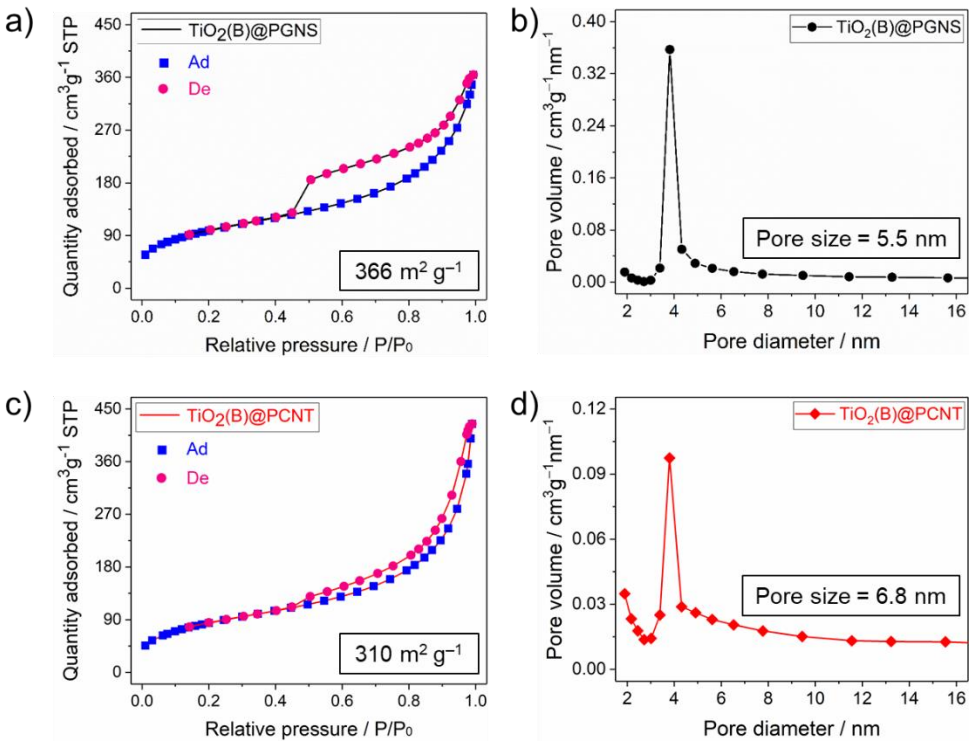

Fig. S5 N_2 adsorption-desorption isotherms and pore size distributions of (a, b) TiO_2(B)@PGNS and (c, d) TiO_2(B)@PCNT nanohybrids. In both cases, typical type-IV hysteresis loops with large BET surface areas (336 m^2 g^{-1} for TiO_2(B)@PGNS, 310 m^2 g^{-1} for TiO_2(B)@PCNT) are observed, implying the presence of uniform channel-like mesopores (5.5 nm for TiO_2(B)@PGNS, and 6.8 nm for TiO_2(B)@PCNT).

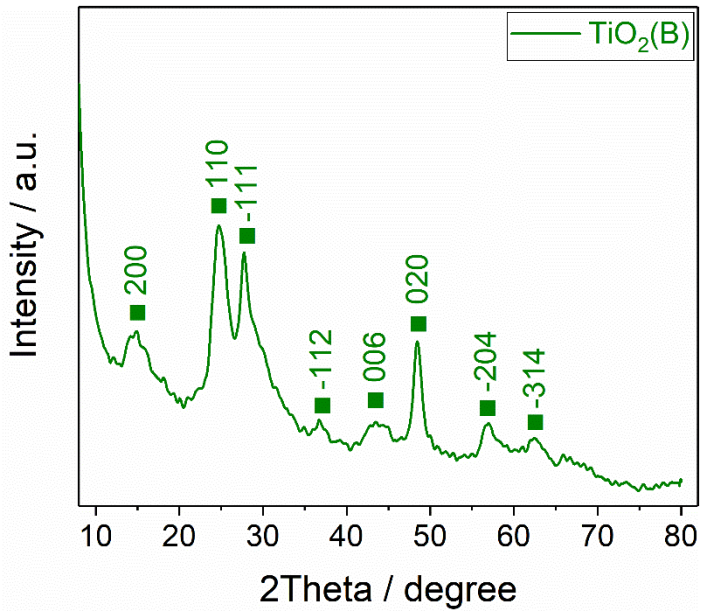

Fig. S6 XRD pattern of TiO_2(B) nanosheets.

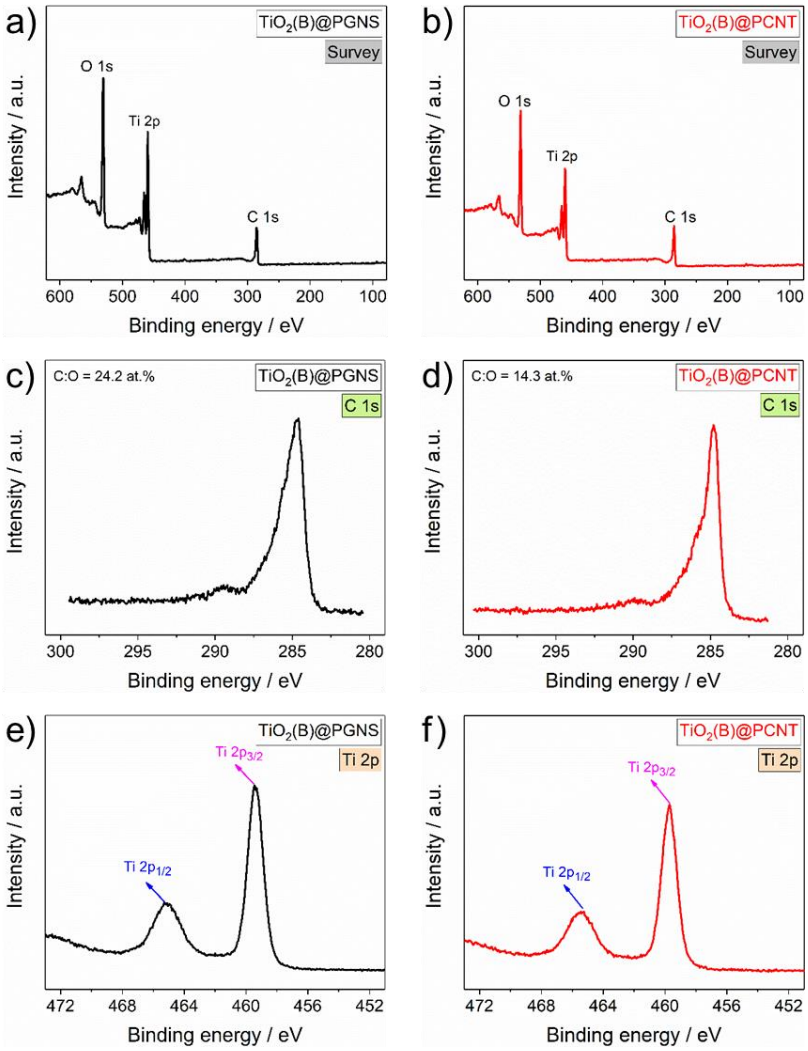

Fig. S7 (a) and (b) Wide-scan survey, (c) and (d) C1s, and (e) and (f) Ti2p XPS spectra of TiO_2(B)@PGNS and TiO_2(B)@PCNT nanohybrids, respectively. It can be seen, in both cases, that small peaks of oxygen-containing groups can be detected and the C:O atomic ratios are extremely high (>14), implying that exceptionally high structural integrity of PGNS and PCNT are well reserved in the nanohybrids. Besides, the peaks assigned to $Ti2p_{1/2}$ and $Ti2p_{3/2}$ of TiO_2(B) can also be clearly distinguished, indicating the successful assembly of TiO_2(B) nanosheets on PGNS and PCNT.[4]

Table S1 TiO_2(B) contents in TiO_2(B)@PGNS and TiO_2(B)@PCNT nanohybrids.

	Atomic percent (%)			TiO_2(B) wt%
	C	**Ti**	**O**	
TiO_2(B)@PG	32.47	22.06	45.46	81.1
TiO_2(B)@PCNT	38.73	19.52	41.75	75.4

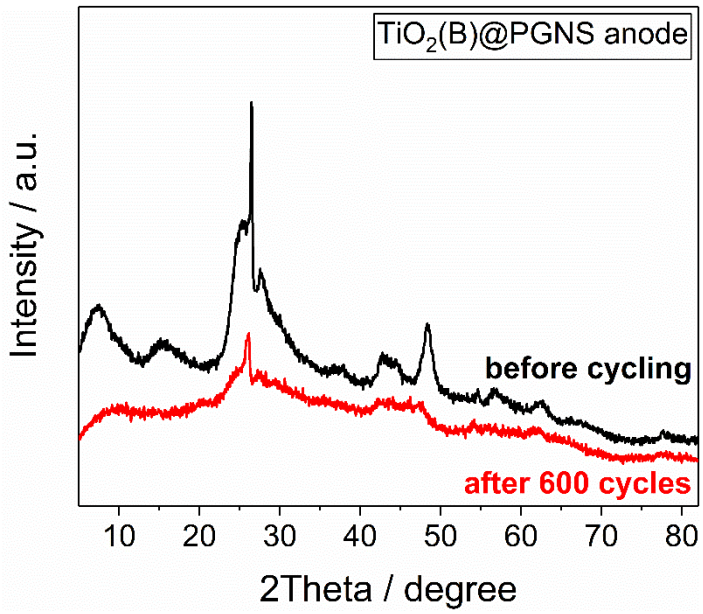

Fig. S8 XRD patterns of TiO_2(B)@PGNS nanohybrids anode before and after cycling.

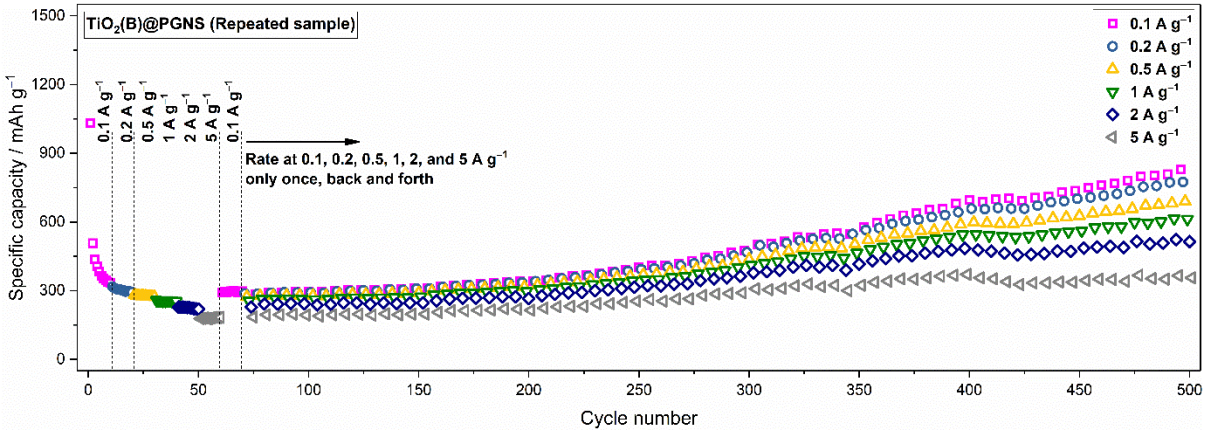

Fig. S9 Repeated rate capability of TiO_2(B)@PGNS nanohybrids.

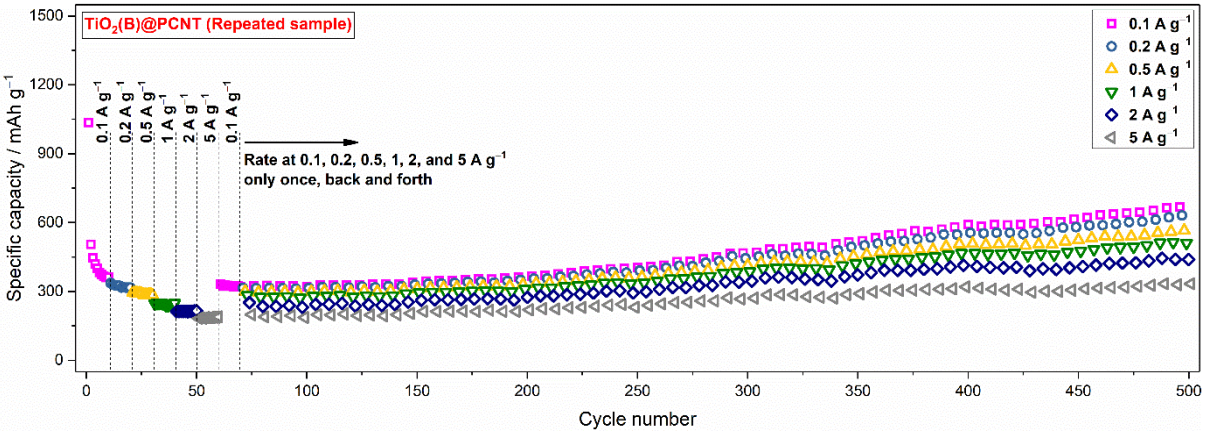

Fig. S10 Repeated rate capability of TiO_2(B)@PCNT nanohybrids.

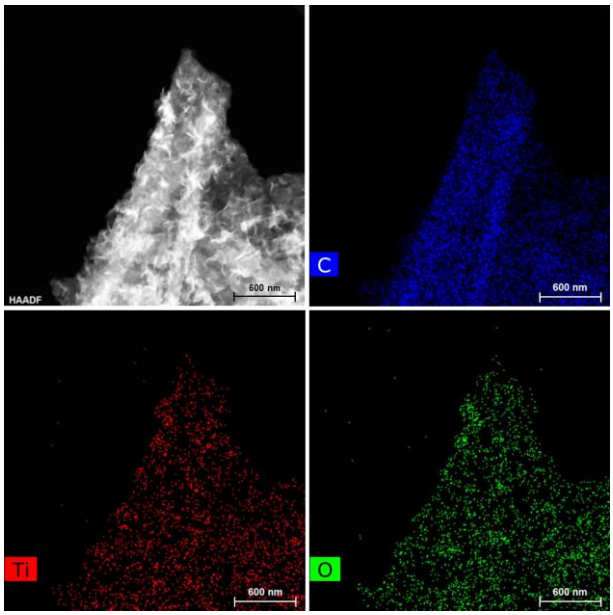

Fig. S11 Dark field TEM image and the corresponding element maps of TiO_2@PGNS nanohybrids after cycling.

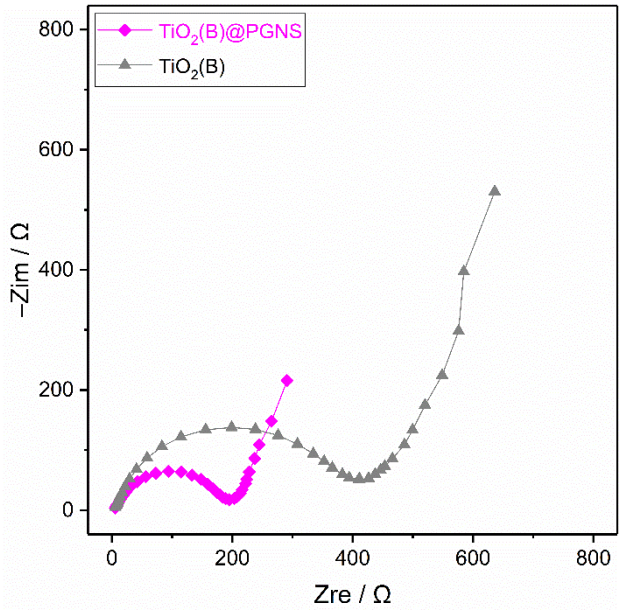

Fig. S12 Nyquist plots of TiO_2(B) nanosheets and TiO_2(B)@PGNS nanohybrids.

References:

1 M. S. Dresselhaus, A. Jorio, M. Hofmann, G. Dresselhaus and R. Saito, *Nano Lett.*, 2010 , **10** , 751–758.

2 Y. Hernandez, V. Nicolosi, M. Lotya, F. M. Blighe, Z. Sun, S. De, I. T. McGovern, B. Holland, M. Byrne, Y. K. Gun'Ko, J. J. Boland, P. Niraj, G. Duesberg, S. Krishnamurthy, R. Goodhue, J. Hutchison, V. Scardaci, A. C. Ferrari and J. N. Coleman, *Nat. Nanotechnol.*, 2008, **3**, 563–568.

3 L. Pan, X.-D. Zhu, X.-M. Xie and Y.-T. Liu, *Adv. Funct. Mater.*, 2015, **25**, 3341–3350.

4 H. Xu, X. D. Zhu, K. N. Sun, Y. T. Liu and X. M. Xie, *Adv. Mater. Interfaces*, 2015, **2**, 1500239.